Journal of Nuclear and Radiochemical Sciences, Vol. 7, No. 1, pp. R13-R18, 2006

Mössbauer Spectroscopy –Nuclear Hyperfine Technique for Studying Dynamic Chemical States of Iron Complexes–

Y. Maeda*

Department of Chemistry, Faculty of Sciences, Kyushu University. Hakozaki 6-10-1, Higashi-ku, Fukuoka, Japan.

Received: October 31, 2005

Mössbauer effect spectroscopy is one of the most important techniques for observing the dynamic phenomena of electronic states in solid. The Mössbauer spectra of mixed valence compounds show relaxation spectra if the electronic states are changed dynamically between Fe^{2+} and Fe^{3+}. The dynamic electronic states of mixed valence compounds are discussed in connection with Mössbauer spectra of $[Fe_2(bpmp)(ppa)_2]X_2$ as examples. The absorption spectra and cyclic voltammograms of the compounds were measured. The electronic states of the mixed compounds are dependent on the species of their anions in the solid state.

1. Introduction

Dinuclear iron complexes with a variety of multidentate ligands have been intensively studied due to the fact that dinuclear iron clusters in the active sites of metalloproteins play important roles such as reversible dioxygen binding and/or activation. Significant examples are haemerythrin,[1-3] the R2 subunit of ribonucleotide reductase,[4] the hydroxylase component of methane monooxygenase,[5-7] and purple acid phosphatase.[8-10] In order to understand the structural and spectroscopic properties of these diiron centers, mixed-valence dinuclear iron (II, III) complexes with a septadentate polypyridine ligand (Hbpmp: 2,6-bis[bis(2-pyridylmethyl)aminomethyl]-4-methylphenol) were synthesized by Suzuki et al.,[11] and diiron (II, III) complexes with the ligands which contain imidazole derivatives instead of pyridine groups (Hbimp),[12] or which contain two phenols substituted for two pyridines[13] were also reported.

The research of "bpmp" complexes is not only to study the properties of model compounds for biological systems in solution, but also to elucidate valence states in the solid state, because the complexes with carboxylic acids having long chains ($CH_3(CH_2)_nCOOH$, $n \geq 3$), show detrapped valence states above 260 K.[14] The rate of electron transfer in solid is sensitive to the packing structure of the solid as the coupling of the electronic state with vibrational coordinates leads to sensitivity to the structure. It should be said that packing structure including the rearrangement of iron moieties of mixed-valence complexes is an important factor in determining the rate of intramolecular electron transfer. In this study mixed-valence μ-phenolate-bis (μ-carboxylate) diiron(II, III) complexes $[Fe_2(bpmp)(ppa)_2](BF_4)_2$ (**1**), $[Fe_2(bpmp)(ppa)_2](ClO_4)_2$ (**2**), $[Fe_2(bpmp)(ppa)_2](PF_6)_2$ (**3**), and $[Fe_2(bpmp)(ppa)_2](BPh_4)_2$ (**4**) are prepared, where "Hppa" represents β-phenylpropionic acid, and the Mössbauer spectra of the complexes are discussed in connection with the electron transfer rates. Chemical structure of $[Fe_2(bpmp)(ppa)_2]^{2+}$ is drawn in Figure 1.

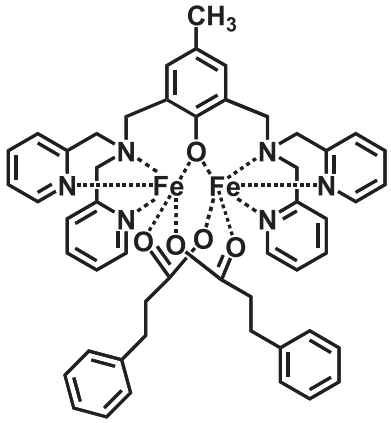

Figure 1. Chemical structure of $[Fe_2(bpmp)(ppa)_2]^{2+}$

*Corresponding author. E-mail: y.maescc@mbox.nc.kyushu-u.ac.jp

2. Experimental

Preparation of 2,6-bis[bis(2-pyridylmethyl)aminomethyl] -4-methylphenol (Hbpmp). Bis(2-pyridylmethyl)amine (2.0 g, 10 mmol) was added dropwise to a solution of 2,6-bis(chloromethyl)-4-methylphenol (1.0 g, 5 mmol) in 50 mL methanol below 10 °C. This solution was stirred for 30 minutes and methanol was removed by evacuation. The residue was dissolved in chloroform and washed twice with water. This chloroform solution was dried over anhydrous sodium sulfate and chloroform was removed by evacuation. The residue was used as Hbpmp (2.6g, 5 mmol).

Preparation of $[Fe^{II}Fe^{III}(bpmp)(ppa)_2](BF_4)_2$ (1). The preparation of **1** is described as a representative example. Synthesis of **1** was carried out in deoxygenated methanol solution under nitrogen atmosphere. A methanol (20 mL) solution of iron(II) tetrafluoroborate (340 mg, 1 mmol) was stirred and added to solution of Hbpmp (260 mg, 0.5 mmol) in methanol (20 mL), and 3-*n*-phenylpropionic acid (140 mg, 1 mmol), and triethylamine (100 mg, 1.0 mmol) was then added. The solution was then exposed to an oxygen atmosphere(air) with stirring. Dark-green precipitates were collected by filtration, washed with ethanol and ether, and dried in vacuum.

Anal. data for $[Fe_2(bpmp)(ppa)_2](BF_4)_2$ (**1**): Calculated for $C_{51}H_{51}N_6Fe_2O_5B_2F_8$: C, 55.02; H, 4.62; N, 7.64; Fe, 10.03. Found: C, 54.64; H, 4.55; N, 7.64; Fe, 9.89%.

Anal. data for $[Fe_2(bpmp)(ppa)_2](ClO_4)_2$ (**2**): Calculated for $C_{51}H_{51}N_6Fe_2O_{13}Cl_2$: C, 53.80; H, 4.51; N, 7.38; Fe, 9.81. Found: C, 53.25; H, 4.54; N, 7.46; Fe, 9.57%.

Anal. data for $[Fe_2(bpmp)(ppa)_2](PF_6)_2$ (**3**): Calculated for $C_{51}H_{51}N_6Fe_2O_5P_2F_{12}$: C, 49.82; H, 4.18; N, 7.64; Fe, 9.08. Found: C, 54.64; H, 4.55; N, 7.64; Fe, 9.28%.

Anal. data for $[Fe_2(bpmp)(ppa)_2](BPh_4)_2$ (**4**): Calculated for $C_{99}H_{91}N_6Fe_2O_5B_2$: C, 75.35; H, 5.81; N, 5.33; Fe, 7.08. Found: C, 74.22; H, 5.88; N, 5.49; Fe, 7.46%.

Microanalysis for carbon, hydrogen, and nitrogen was car-

Published on Web 06/30/2006

ried out at the Elemental Analysis Center, Kyushu University. Quantitative analysis for iron was performed by atomic absorption analysis, using an Atomic Absorption / Flame Emission Spectrometer AA-625-11 (Shimadzu).

Physical Measurements. Absorption and reflection spectra were measured using a Shimadzu UV-3100PC self-recording spectrophotometer in the region from 400 to 2000 nm.

Cyclic voltammetry of the complexes in acetonitrile was carried out on an AC/DC Cyclic Polarograph P-900 (Yanaco) at 293 K under argon atmosphere. A standard three-electrode system(BAS) was employed comprising a glassy carbon working electrode, a Ag-Ag^+-MeCN-NBu_4ClO_4 (RE-5, BAS), reference electrode and a platinum counter electrode in the region from −500 to 1200 mV. Ferrocene was used as a standard. The observed values for the complexes were converted to redox potentials versus SCE by using the following equation.

Redox potential for the complexes

= observed value for a complex − observed value for Ferrocene + 0.0739 (Ferrocene *vs.* Ag / AgCl) + 0.272 (Ag / AgCl *vs.* SCE) V. (1)

The Mössbauer spectra were measured using a Topologic Mössbauer spectrometer with a ^{57}Co/Rh source in the transmission mode. All isomer shifts are given relative to the center of a spectrum for α-Fe at room temperature. The temperature was controlled over 80 – 295 K using an Oxford Intelligent temperature controller or over 5 – 295 K using a Lakeshore 331 temperature controller, and a Kenwood Regulated DC power supply. The spectra were fitted by a Lorentzian line shape using a software of IGOR PRO (Wave Metrics Inc.) on a personal computer.

3. Results and Discussion

Reflection and Absorption Spectra. Absorption spectra of complexes **1** – **4** in acetonitrile solution were measured. An absorption spectrum of **4** in acetonitrile solution is displayed in Figure 2 as a representative example. The complexes give absorption bands in the visible region: λ=561 nm, ε=931 $dm^3cm^{-1}mol^{-1}$ for **1**, λ=565 nm, ε=981 $dm^3cm^{-1}mol^{-1}$ for **2**, λ=561 nm, ε=1050 $dm^3cm^{-1}mol^{-1}$ for **3**, and λ=539 nm, ε=1108 $dm^3cm^{-1}mol^{-1}$ for **4**. These are assigned to charge transfer transitions from the pπ orbital of a bridging phenolato group to the half filled dπ* orbital of Fe^{III} ions.[11] The ligand field bands may be obscured under the above CT band.

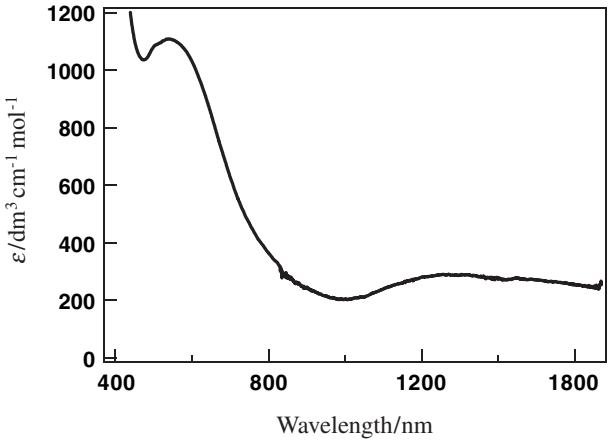

Figure 2. Absorption spectrum of **4** in acetonitrile solution(1×10^{-3} mol)

Complexes **1** – **4** show an additional broad absorption band in near-IR region. The band is unambiguously assigned to the intervalence charge transfer transition (IT) of the mixed-valence complexes. The properties associated with these IT bands for complexes **1** – **4** are collected in Table 1. The energy of the optical transition (ν_{max}) for the IT band of complex **1** is 7794 cm^{-1} and the width of half maximum ($\Delta\nu_{1/2}$) is 4661 cm^{-1}. The $\Delta\nu_{1/2}$ value is compared to the theoretical value of 4243 cm^{-1} calculated by eq 1. The ratio of $\Delta\nu_{1/2}$ (obsd) / $\Delta\nu_{1/2}$ (theor) = 1.1 is commonly found for weakly to moderately coupled binuclear mixed-valence dimers.

$$\Delta\nu_{1/2}\,(\text{theor}) = (2.31\times10^3\nu_{max})^{1/2} \quad (1)$$

The electron delocalization coefficient α in a mixed-valence system is given by eq 2[15] where ε_{max} is the molar extinction coefficient of the IT band and *d* is the distance (Å) between two metal centers associated with the IT transition. The α^2 value of 0.0065 (α = 0.081) is evaluated for complex **1** using the *d* = 3.36 Å,[14,16] ν_{max} = 7794 cm^{-1}, $\Delta\nu_{1/2}$ = 4661 cm^{-1}, and ε_{max} = 289 $dm^3\,cm^{-1}\,mol^{-1}$.

$$\alpha^2 = \frac{4.24\times10^{-4}\varepsilon_{max}\Delta\nu_{1/2}}{\nu_{max}d^2} \quad (2)$$

Therefore, the mixed-valence bpmp complex **1** belongs to Class II in the classification of Robin and Day[17] on the base of the Mössbauer spectra described later. The resonance energy matrix element arising from orbital overlap between electron donor and acceptor sites, H_{ab} can be calculated from eq 3 to yield 631 cm^{-1} (7.5 kJ mol^{-1}).[18] The thermal free energy of electron transfer, ΔG^*, for a symmetrical mixed-valence complex is given to be 15.8 kJ mol^{-1} by eq 4.[19]

$$H_{ab} = \alpha\cdot\nu_{max} \quad (3)$$

$$\Delta G^* = \frac{\nu_{max}}{4} - H_{ab} \quad (4)$$

The thermal rate constant for electron transfer is obtained by eq 5.[15]

$$k_{et} = \nu_{et}\exp\left(\frac{-\Delta G^*}{RT}\right) \quad (5)$$

$$\nu_{et} = \left(\frac{2\pi^{3/2}H_{ab}}{\hbar}\right)(kT\nu_{max})^{-1/2} \quad (6)$$

The ν_{et} term given by eq 6 is the frequency factor for electron transfer. The calculated value of k_{et} for complex **1** is 3.8×10^{14} s^{-1}. The same arguments can be applied to complexes **2** – **4**. The calculated values of k_{et} are similar to each other. Creutz has pointed out that, in a series of mixed-valence $[Ru(bpy)_2Cl]_2L$ complexes (where bpy is 2,2'-bipyridine and L is the bridging ligand), there is a 100 fold increase in k_{et} from 10^7 to 10^9 s^{-1} as the metal-metal distance decreases from ~14 to ~7 Å.[17] Using this trend as a qualitative guide, it is not surprising that the k_{et} values obtained for complex **1 – 4** are ~10^{14} since

Table 1: Spectrochemical Properties of the Mixed-valence Complexes.

Comp.	ν_{max}/cm^{-1}(ε/$dm^3cm^{-1}mol^{-1}$)	$\Delta\nu_{1/2}$(obs)/cm^{-1}	$\Delta\nu_{1/2}$(theo)/cm^{-1}	α^2	H_{ab}/cm^{-1}	ΔG*/ kJ mol^{-1}	k_{et}/s^{-1}
1	7794 (289)	4661	4243	0.0065	631	15.8	3.8×10^{14}
2	7764 (282)	4453	4235	0.0061	606	16.0	3.5×10^{14}
3	7770 (251)	4628	4237	0.0056	583	16.3	3.2×10^{14}
4	7782 (288)	4695	4240	0.0065	630	15.8	3.8×10^{14}

the triply bridged diiron units in the complexes have relatively short Fe–Fe distances (~3.4 Å).

Cyclic Voltammetry. Cyclic Voltammograms of the complexes were measured in acetonitrile at 293 K and are shown in Figure 3. Two quasi-reversible waves corresponding to $Fe^{II}Fe^{II}$ / $Fe^{II}Fe^{III}$, E_1 (V vs. SCE) and $Fe^{II}Fe^{III}$ / $Fe^{III}Fe^{III}$, E_2 (V vs. SCE), couples are observed. The potentials observed for the complexes are E_1=−0.089 V and E_2=0.646 V for **1**, and E_1= −0.094 V and E_2=0.631V for **2**, E_1=−0.084 V and E_2=0.641 V for **3**, and E_1=−0.104 V and E_2=0.611 V for **4**, being similar to those observed for other $[Fe_2(bpmp)L_2](BF_4)_2$ complex.[14,19]

The redox potentials of the complexes are dependent on the species of carboxylic acid. Peak-to-peak separations of these two waves are 715 – 735 mV, and the ratios of the oxidation currents (i_{pa}) for the forward scan to the reduction currents (i_{pc}) for the reverse scan were close to unity for the both couples. From the separation of the redox potentials of E_1 and E_2, comproportionation constants K_c (at 20 ˚C) of the following reaction are calculated from eq 7.

$$(Fe^{III}-Fe^{III}) + (Fe^{II}-Fe^{II}) \rightleftarrows 2\,(Fe^{II}-Fe^{III})$$
$$E_2 - E_1 = RT/F\ln K_c \qquad (7)$$

The E values of the $Fe^{II}Fe^{III}$ bpmp complexes are well correlated with the electron donor ability of the bridging carboxylates; the complexes with carboxylic acids of the weak donor ability is prefer low oxidation states. Equation 7 demonstrates that the thermodynamic significance of peak separation of the waves is its relationship to the comproportionation equilibrium constant. The larger separation of the waves indicates the substantial stability of the diiron(II, III) ion over its corresponding diiron(II, II) and diiron(III, III) species. For complexes **1** – **4**, K_c values calculated from eq 7 are 2.87×10^{12}, 1.94×10^{12}, 1.94 $\times 10^{12}$, and 1.31×10^{12}, respectively. Therefore, in complexes **1** – **4**, mixed-valence states are highly stabilized in acetonitrile solution.

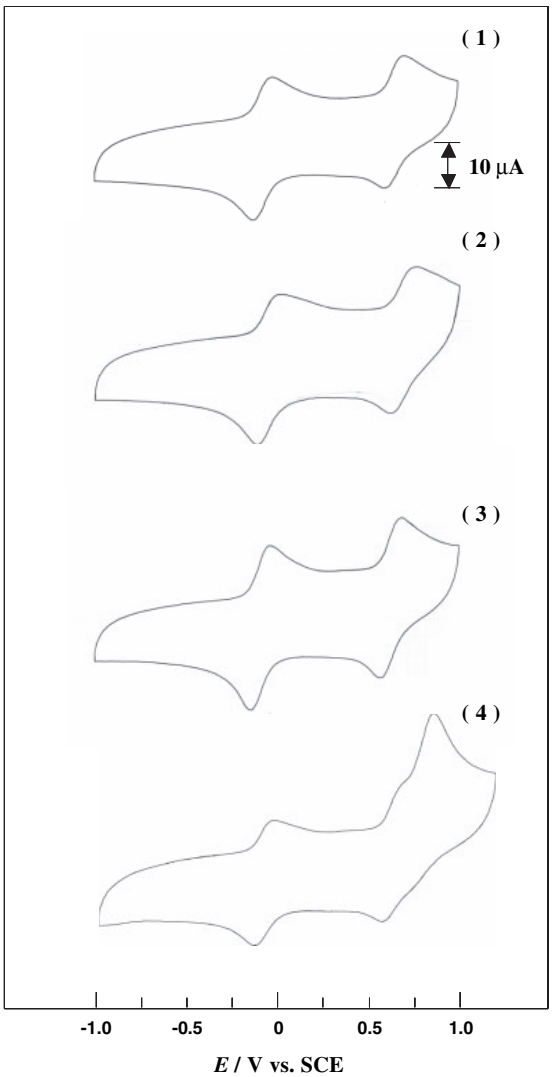

Figure 3. Cyclic voltammograms of the complexes **1**–**4**.

Mössbauer spectroscopy. The Mössbauer spectra for the complexes were measured at various temperatures. The good fits of the spectra to four Lorentzian line shapes for complex **1** were obtained at all temperatures. Each spectrum consists of two doublets. One of the two doublets at 80 K is characteristic of high-spin Fe^{II} with an isomer shift (δ) of 1.14 mm s^{-1} and a quadrupole splitting (Δ) of 2.75 mm s^{-1}. The other is characteristic of high-spin Fe^{III} with δ of 0.48 mm s^{-1} and Δ of 0.56 mm s^{-1}. The area ratios of the two doublets are nearly 1:1. Upon increasing temperature, the two doublets approach each other but still remain even at 295 K. The δ and Δ values for high-spin Fe^{II} at 295 K are 0.83 mm s^{-1}, 1.27 mm s^{-1}, and those for high-spin Fe^{III} 0.57 mm s^{-1}, 0.75 mm s^{-1} , respectively. The area ratios of two doublets are 1:1. The result of the Mössbauer spectra of complex **1** was comparable to that reported previously.[16,20] The temperature dependence of the Mössbauer parameters of complex **1** are plotted in Figures 4a and 4b with those for other complexes.

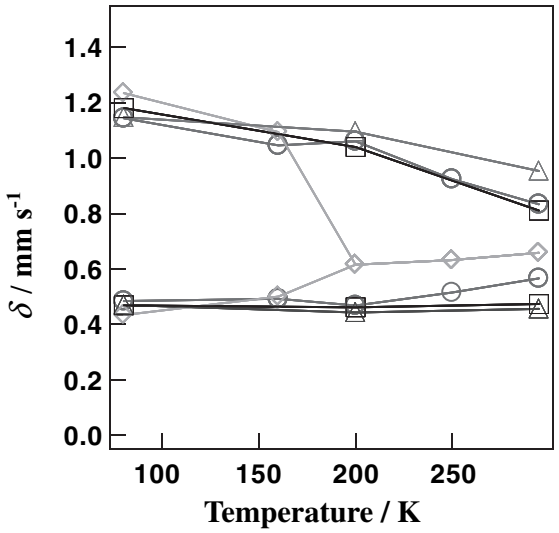

Figure 4a. Plots of the isomer shift vs. temperature for complexes **1**–**4**. Complex **1** (○), complex **2** (△), complex **3** (□), and complex **4** (◇).

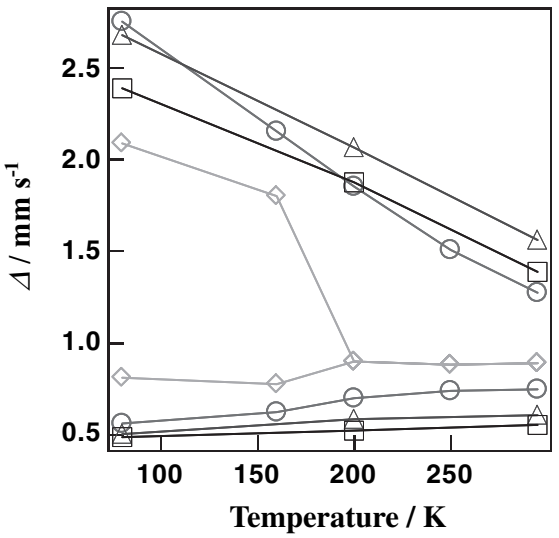

Figure 4b. Plots of the quadrupole splitting vs. temperature for complexes **1**–**4**. Complex **1** (○), complex **2** (△), complex **3** (□), and complex **4** (◇).

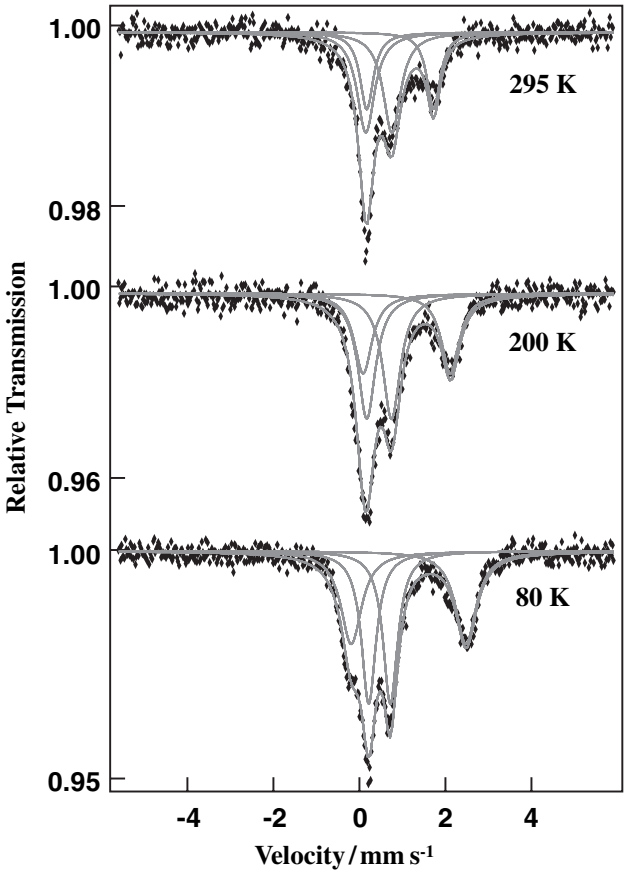

Figure 5. Temperature dependence of the Mössbauer spectra of complex **2**.

The Mössbauer spectra of complex **2** are illustrated in Figure 5. The Mössbauer spectra of complex **3** are similar to those of complex **2.** The Mössbauer spectra of complexes **2** and **3** at 80 K clearly show the characteristic Fe^{II} and Fe^{III} doublets in an area ratio of 1:1. At 295 K, complex **2** exhibits two doublets assigned to high-spin Fe^{II} and Fe^{III} with nearly equal area ratio. On the other hand, the Mössbauer spectrum of complex **3** at 295 K exhibits two doublets assigned to high-spin Fe^{II} and Fe^{III} with a different area ratio. The area ratio of Fe^{II} and Fe^{III} is about 3:7. It is not easy to believe that this unequal area ratio results entirely from a difference in the temperature dependence of the recoilless fraction of Fe^{III} to Fe^{II} sites in these materials. Rather, it is proposed that the difference is due to the analytical error for asymmetric absorption or due to a texture effect in the sample.[21,22] Unfortunately, it is difficult to analyze the spectra with an asymmetric doublet of Fe^{II} and a symmetric doublet of Fe^{III}, but the temperature dependence of δ and Δ are similar to those observed for typical valence trapped compounds.[16]

The Mössbauer spectra of complex **4** are shown in Figure 6. Compared to the Mössbauer spectra of complexes **1 – 3**, the spectra of complex **4** are considerably different. At 80 K, the spectrum is composed of two doublets assigned to Fe^{II} and Fe^{III} sites. The δ and Δ values are 1.23 mm s^{-1} and 2.09 mm s^{-1} respectively, for Fe^{II} site, and 0.43 mm s^{-1}, 0.81 mm s^{-1}, respectively, for Fe^{III} site. As the temperature is increased, these two doublets gradually approach each other with line broadening to become a single average-valence doublet. The Mössbauer spectrum at 295 K shows single average-valence doublet with δ of 0.66 mm s^{-1} and Δ of 0.89 mm s^{-1}. The values of the δ and Δ are comparable to valence detrapped bpmp complexes reported previously.[14,23] However, the area ratio of Fe^{II} and Fe^{III} is not equal at 80 K. The area ratios of Fe^{II} and Fe^{III} at 80 K in complex **4** are 3:7. Also, Δ value of Fe^{III} site at 80 K, 0.81 mm s^{-1}, is relatively high as a high-spin Fe^{III} species. Upon decreasing

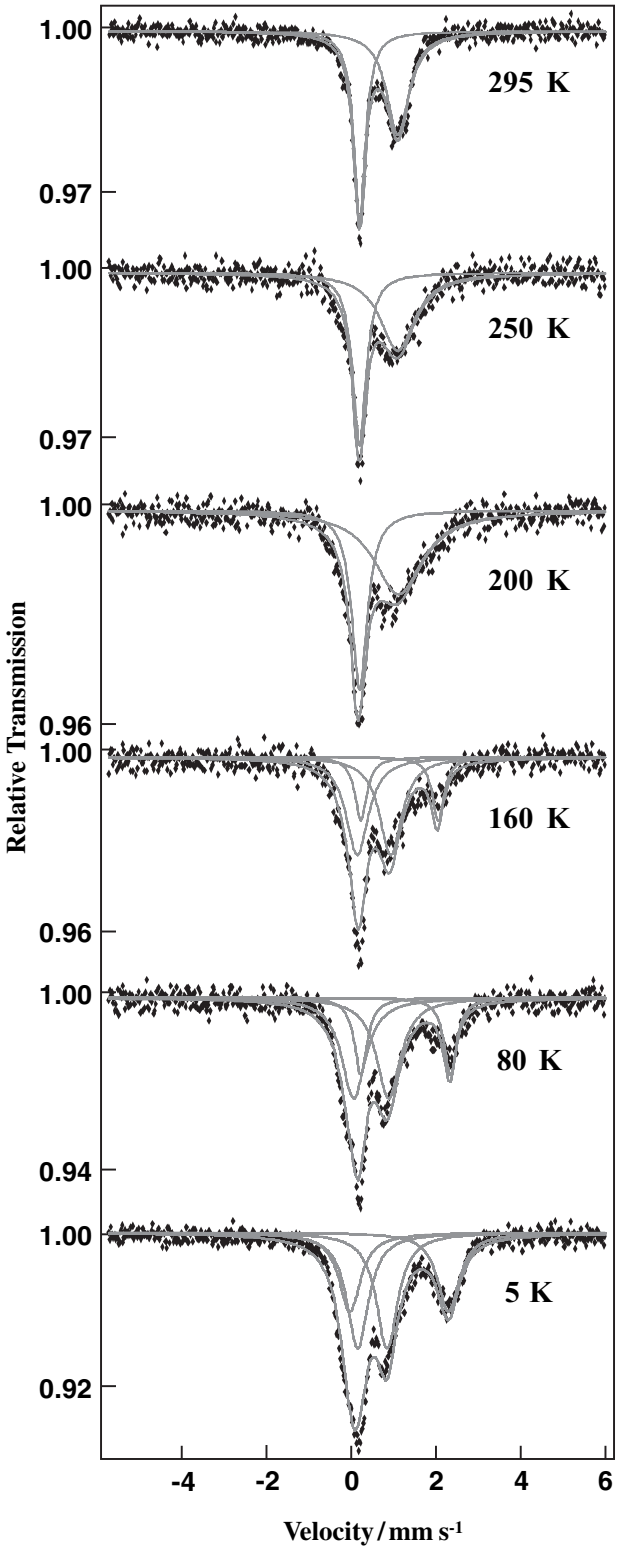

Figure 6. Temperature dependence of the Mössbauer spectra of complex **4**.

the temperature from 80 K, the area ratios of Fe^{II} and Fe^{III} gradually approach to 1:1. The area ratio of Fe^{II} and Fe^{III} at 5 K is nearly 1:1. The δ value and Δ value for Fe^{II} is 1.13 mm s^{-1} and 2.33 mm s^{-1} and those for Fe^{III} is 0.50 mm s^{-1} and 0.69 mm s^{-1}, respectively. This result indicates that valence detrapping occurs in complex **4** even at 80 K, and the valences are trapped at 5 K. It is concluded that the valence delocalization in complex **4** takes place at the lowest temperature in the bpmp mixed-valence complexes studied until now. No bpmp mixed-valence complexes which show valence detrapping at 80 K have been reported previously.[24]

The Mössbauer spectra of complexes **1 – 4** at 295 K are illustrated in Figure 7 to compare the differences of electron

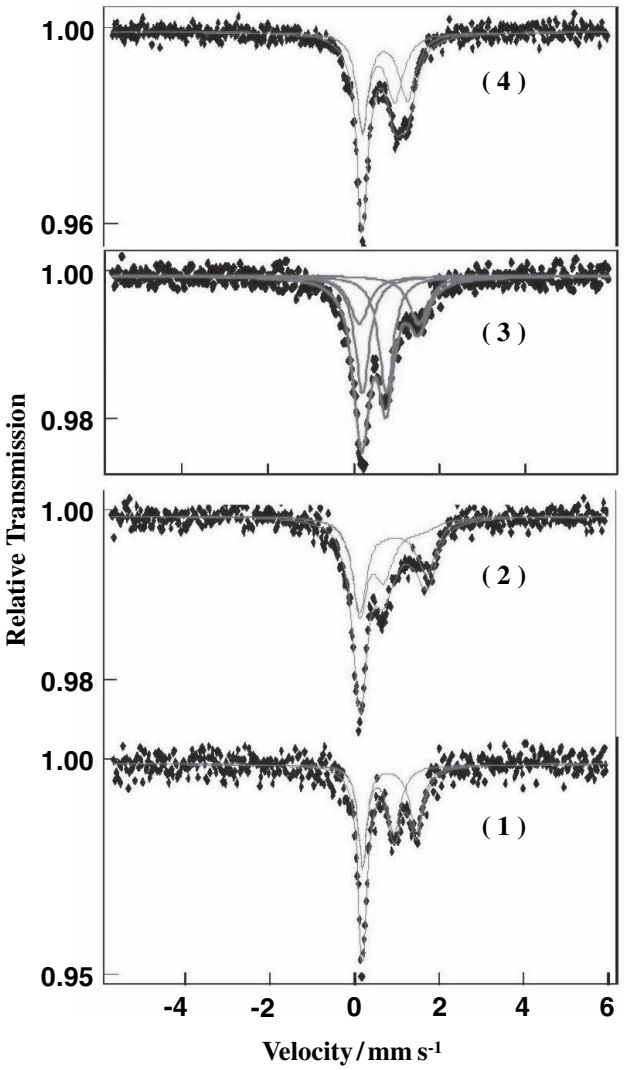

Figure 7. Mössbauer spectra for complexes **1**–**4** at 295 K. The solid lines represent theoretical fits obtained by the two-site relaxation model.

transfer rate. Figure 7 and the results of the Mössbauer fitting parameters clearly show the electron transfer rate of $[Fe_2(bpmp)(ppa)_2]^{2+}$ cations is sensitive to the species of counter anions. Hendrickson et al. reported the sensitivities of anions to mixed-valence bimp complexes.[12] $[Fe_2(bimp)(AcO)_2]^{2+}$ (where AcO = acetate anion) shows a completely valence detrapped Mössbauer spectrum at 290 K when anions are BF_4^-. The ClO_4^- salt shows valence trapped spectrum even at 350 K. They concluded that the change in the counter anions can affect the rate of electron transfer of mixed-valence complexes because of the consequence of the vibronic nature of the $Fe^{II}Fe^{III}$ center. If there are appreciable intermolecular interactions between cations and anions in the crystals of $Fe^{II}Fe^{III}$ complexes, then these interactions will tend to trap the valence. The complex will not have enough thermal energy to make an interconversion between two vibronic states of $Fe_A^{II}Fe_B^{III}$ and $Fe_A^{III}Fe_B^{II}$, overcoming interactions with neighboring molecules in the crystal. However, if the thermal energy is large enough to overcome the interactions or the interactions are weakened by changing in anions, complexes show the valence detrapped states.

In order to interpret the Mössbauer spectra of the complexes, theoretical Mössbauer spectra are calculated by considering a relaxation model. The mathematical formalism which is applied to this relaxation model is based on the quantum mechanical density matrix equations of motion (dG_i/dt) given by Wickmann.[25,26] The detail of the model and the fitting is described elsewhere.[25,26] The probability of keeping Fe^{II} electronic state at site A is nearly 0.8 and this result indicates that an excess electron stays 80% of the time at site A and 20% of the time at site B in complex **1**. Therefore valence state of complex **1** is $Fe^{2.2+}Fe^{2.8+}$ at 295 K in Mössbauer timescale. This unusual valence state of complex **1** is also reflected in the temperature dependence of δ and Δ as shown in Figures 4a and 4b. Temperature dependence of δ and Δ of complexes **2** and **3** exhibits typical behavior of valence trapped process between 80 K and 295 K.[16] The δ of high-spin Fe^{III} usually decrease with increasing temperature except for complexes which experience a phase transition in the temperature measured, but δ of Fe^{III} site in complex **1** increases with increase in temperature, and the Δ of high-spin Fe^{III} are usually invariant with increase in temperature. However the Δ of complex **1** increase with increase in temperature. The line broadening of spectra, usually observed in the valence detrapping process, was not observed in complex **1,** and area ratios of Fe^{II} and Fe^{III} remain 1:1 for all measured temperatures. Therefore, from theoretical fittings of the spectra, complex **1** takes the unusual valence state of $Fe^{2.2+}Fe^{2.8+}$ at 295 K in the Mössbauer timescale.

On the other hand, Mössbauer spectra of complex **2** exhibit typical valence trapped spectra. The temperature dependence of δ and Δ are typical behavior of valence trapped complexes and theoretical results of $\tau = 1.3 \times 10^{-6}$ s reflects that the electron transfer rate is slower than the Mössbauer timescale. The same arguments can be applied to complex **3**, and thus the theoretical fits of complex **3** are unreliable because the area ratio of Fe^{II} and Fe^{III} for complex **3** is not equal at 295 K.

Compared to other complexes, complex **4** at 295 K shows faster electron transfer than the Mössbauer timescale and only an average spectrum is observed. Theoretical fitting of complex **4** describes $\tau = 2.9 \times 10^{-8}$ s at 295 K. As shown in Figure 6, line broading of spectra are observed with increasing the temperature and the two doublets converged together above 200 K. This behavior of the spectra is observed in valence detrapping processes and thus the complex **4** exhibits a valence trapped to valence detrapped transition between 5 K and 295 K in Mössbauer timescale.

Reference

(1) A. L. Feig and S. J. Lippard, Chem. Rev. **94,** 759 (1994).
(2) R. E. Stenkamp, L. C. Sieker, L. H. Jensen, and J. Sanders-Loehr, Nature(London) **291**, 263 (1981); R. E. Stenkamp, L. C. Sieker, and L. H. Jensen, J. Am. Chem. Soc. **106**, 618 (1984).
(3) P. C. Wilkins and R. G. Wilkins, Coord. Chem. Rev. **79**, 195 (1987); R. G. Wilkins and P. C. Harrington, Adv. Inorg. Biochem. **5,** 51 (1983).
(4) L. Yhelander and P. Reichard, Annu. Rev. Biochem. **48**, 133 (1979); P. Reichard and A. Ehrenberg, Science **221**, 514 (1987); B. M. Sjöberg, T. M. Loehr, and J. Sanders-Loehr Jr., J. Biochem. **21**, 96 (1982).
(5) J. G. Dewitt, J. G. Bensten, A. C. Rosenzweig, B. Hedman, J. Green, S. Pilkington, G. C. Bensten, G. C. Papaefthymiou, H. Dalton, K. O. Hodbson, and S. J. Lippard, J. Am. Chem. Soc. **113**, 9219 (1991).
(6) B. G. Fox, W. A. Froland, J. E. Dege, and J. D. Lipscomb, J. Biol. Chem. **264**, 10023 (1989).
(7) M. P. Woodl and H. Dalton, J. Biol. Chem. **259**, 53 (1984).
(8) B. A. Averill, J. G. Davis, S. Burman, T. Zirino, J. Sanders-Loehr, T. M. Loehr, J. T. Sage, and P. G. Debrunner, J. Am. Chem. Soc. **109**, 3760 (1987); S. M. Kauzlarich,. B. K. Teo, T. Zirino, S. Burman, J.C. Davis, and B. A. Averill, Inorg. Chem. **25**, 2781 (1986).
(9) E. Sinn, G. J. O'Connor, J. de Jersey, and B. Zerner, Inorg. Chim. Acta **78**, L13 (1983).
(10) B.C. Antanaitis and P. Aisen, Adv. Inorg. Biochem. **5**, 111 (1983).
(11) M. Suzuki, A. Uehara, H. Oshio, K. Endo, M. Yanagi, S.

Kida, and K. Saito, Bull. Chem. Soc. Jpn. **60**, 3547 (1987); M. Suzuki, A. Uehara, H. Oshio, K. Endo, M. Yanagi, S. Kida, and K. Saito, Bull. Chem. Soc. Jpn. **61**, 3907 (1988).

(12) A. S. Borovik, B. P. Murch, and L. Que Jr., J. Am. Chem. Soc. **109**, 7190 (1987); M. S. Mashuta, R. J. Webb, K. J. Oberhausen, J. F. Richardson, R. M. Buchanan, and D. N. Hendrickson, J. Am. Chem. Soc. **111**, 2745 (1989); M. S. Mashuta, R. J. Webb, J. K. McCusker, E. A. Schmitt, K. J. Oberhausen, J. F. Richardson, R. M. Buchanan, and D. N. Hendrickson, J. Am. Chem. Soc. **114**, 3815 (1992); A. S. Borovik and L. Que Jr., J. Am. Chem. Soc. **110**, 2345 (1988).

(13) A. Neves, M. A. de Brito, I. Vencato, V. Drago, K. Griesar, and W. Haase, Inorg. Chem. **35**, 2360 (1996); C. Belle, I. Gautier-Luneau, J. -L. Pierre, and C. Scheer, Inorg. Chem. **35**, 3706 (1996).

(14) Y. Maeda, Y. Tanigawa, S. Hayami, and Y. Takashima, Chem. Lett. **1992**, 591 (1992); Y. Maeda, Y. Tanigawa, N. Matsumoto, H. Oshio, M. Suzuki, and Y. Takashima, Bull. Chem. Soc. Jpn. **67**, 125 (1994); Y. Maeda, Y. Tanigawa, Y. Ando, Y. Takashima, and N. Matsumoto, Acta Chim. Hungarica, Models in Chem. **130**, 55 (1993).

(15) A. S. Borovik, V. Papaefthymiou, L. F. Taylor, O. P. Anderson, and L. Que Jr., J. Am. Chem. Soc. **111**, 6183 (1989); T. Meyer, J. Chem. Phys. Lett. **64**, 417 (1979); J. Hopfield, J. Proc. Natl. Acad. Sci. U.S.A. **71**, 3640 (1974); N. R. Kestner, J. Logan, and J. Jortner, J. Phys. Chem. **78**, 2148 (1974).

(16) T. Manago, S. Hayami, H. Oshio, S. Osaki, H. Hasuyama, R. H. Herber, and Y. Maeda, J. Chem. Soc. Dalton Trans. **1999**, 1001 (1999).

(17) M. B. Robin and P. Day, Adv. Inorg. Chem. Radiochem. **10**, 247 (1967).

(18) N. S. Hush, Prog. Inorg. Chem. **8,** 391 (1967).

(19) C. Creutz, Prog. Inorg. Chem. **30**, 1 (1983).

(20) T. Manago, S. Hayami, and Y. Maeda, J. Radioanal. Nucl. Chem. **239**, 267 (1999).

(21) G. S. Matouzenko, A. Bousseksou, S. A. Borshch, M. Perrin, S. Zein, L. Salmon, G. Molnar, and S. Lecocq, Inorg. Chem. **43**, 227 (2004).

(22) J. P. Martin, J. Zarembowitch, A. Bousseksou, A. Dworkin, J. G. Haasnoot, and F. Varret, Inorg. Chem. **33**, 6325 (1994).

(23) T. Kambara, D. N. Hendrickson, M. Sorai, and S. M. Oh, J. Chem. Phys. **85**, 2895 (1986).

(24) Y. Maeda, A. Ishida, M. Ohba, S. Sugihara, and S. Hayami, Bull. Chem. Soc. Jpn. **75**, 2441 (2002).

(25) H. H. Wickman, *Mössbauer Effect Methodology*, Ed. I. J. Gruverman, Plenum, New York Vol. **2**, 39 (1966).

(26) H. H. Wickman, M. P. Klein, and D. A. Shirley, Phys. Rev. **152**, 345 (1966).